Experimental Study and Simulation of Different EOR Techniques in a Non-Fractured Carbonate Core from an Iranian Offshore Oil Reservoir

Jafari, Mahdi; Badakhshan, Amir; Taghikhani, Vahid*+; Rashtchian, Davood; Ghotbi, Cirous

Department of Chemical and Petroleum Engineering, Sharif University of Technology, Tehran, I.R. IRAN

Sajjadian, Vali Ahmad

Arvandan Company, National Iranian Oil Company, Tehran, I.R. IRAN

ABSTRACT: *In this research the experimental and theoretical studies on different Enhanced Oil Recovery (EOR) techniques, i.e. Water Flooding (WF), Gas Injection (GI) and Water Alternating Gas process (WAG) were performed on specimens taken from an Iranian carbonate offshore reservoir at the reservoir condition. The experimental results for each specified techniques were compared with the corresponding results obtained from a simulation model. In the case of WF and GI, the injection rates were set to be 0.1, 0.2 and 0.5 cc/min while for the WAG experiments, with two WAG ratios 1 and 2 and with 7, 7, and 10 cycles, the injection rates were 0.1, 0.2 and 0.5 cc/min. The results obtained from the experiments revealed that in all cases the amount of recovered oil is increased. Furthermore, the results showed that increase in the recovery of oil is significant in the case of the WAG injection with optimum rate of injection fluids comparing to those of the WF and GI scenarios. It was also pronounced that the recovery of oil with WAG ratio 2 is more than that with ratio 1. It should be mentioned that samples for sea water and pure methane were considered to be as injection fluids. It was also shown that the experimental results can be accurately correlated with a black oil numerical simulator, Eclipse100.*

KEY WORDS: *WAG, Water flooding, Gas injection, Core flooding, Fingering, Mobility ratio.*

INTRODUCTION

After primary and secondary recovery such as Water Flooding (WF) and Gas Injection (GI) millions of barrels of oil still remains in trapped form in the reservoirs. Water Alternating Gas (WAG) injection as a tertiary recovery method is one of the Enhanced Oil Recovery (EOR) methods which have recently received a great deal of attention. The first WAG implementations were reported in 1957 in Canada, the United States and the

* To whom correspondence should be addressed.
+ E-mail: taghikhani@sharif.edu
1021-9986/08/2/81 11/$/3.10

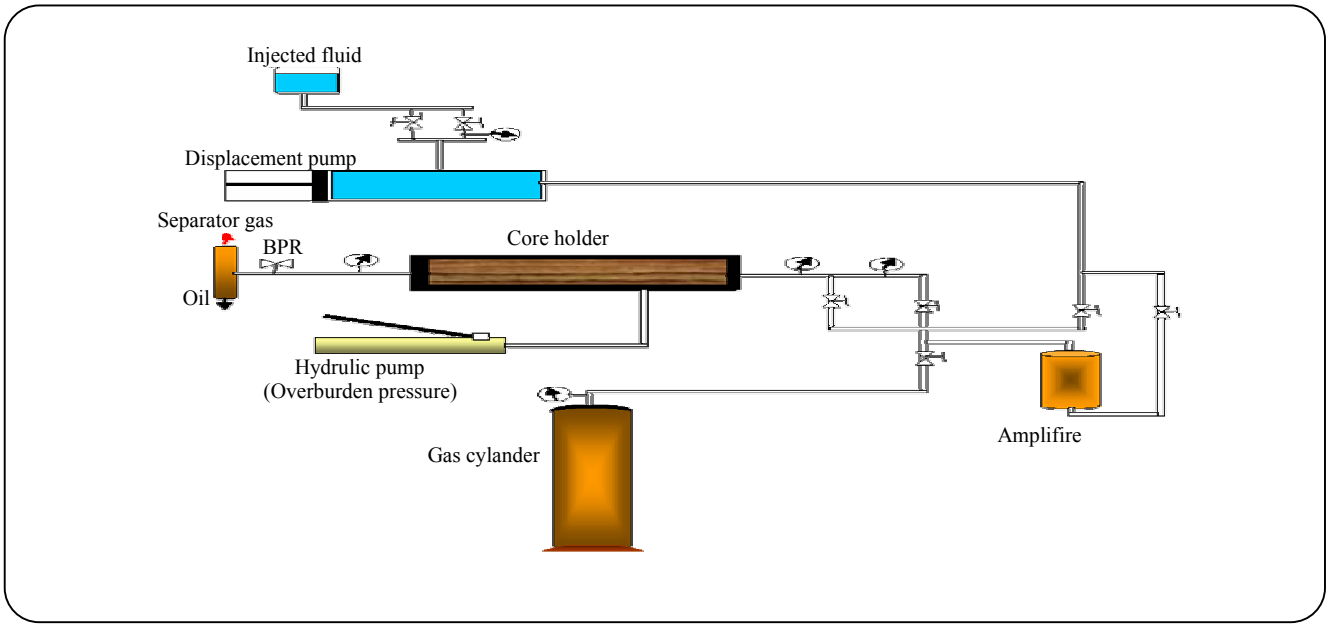

Fig. 1: Schematic diagram for the core flooding apparatus used in the experiments.

North Sea [1]. The WAG process can be implemented in both onshore and offshore reservoirs with hydrocarbon or non-hydrocarbon gases as injection fluids. It has been shown that implementation of the WAG process can lead to an increase in oil recovery ranging from 5 to10 percent of the Initial Oil in Place (IOIP) [2]. Also using the WAG process the well-known shortcoming of the conventional WF and GI processes, i.e., gas fingering and mobility ratio problems can be overcome and, in turn, result in a stable and uniform frontal displacement. As reported before, the WAG injection has an intrinsic potential to increase the macroscopic efficiency in immiscible oil displacement as well as the microscopic efficiency in miscible oil displacement. So far several types of the WAG processes have been used such as Miscible WAG (MWAG) [3-7], Immiscible WAG (IWAG) [8-9], Hybrid WAG (HWAG) [10-14], Simultaneous WAG (SWAG) [15-18], Foam WAG (FAWAG) and Water Alternating Steam Process (WASP) [19]. In the field scales the WAG process has been used in sandstone reservoirs to a large extent but rarely in the carbonate reservoirs [2]. It would be worth noting that the offshore reservoirs could be a good candidate for the implementation of the WAG process due to the availability of sea water. In Iran there are a number offshore reservoirs, which can be considered as appropriate candidates for the implementation of the WAG technique for tertiary recovery in field scale. In this research the WF, GI and WAG processes were studied on core samples taken from an Iranian offshore reservoir at reservoir conditions. The effect of parameters on the amount of oil recovered such as the rate of injection of fluids optimum ratio and cycle for in the case of the WAG experiments were studied.

EXPERIMENTAL

Apparatus

In order to carry out the core flooding experiments a high-pressure core flooding apparatus was used. A schematic diagram of the core flooding system along with its ancillaries, obtained from Eksir Daroo Manufacturing Company, is shown in Fig. 1. This apparatus consists of; an accurate high temperature controlled air bath with accuracy of ± 0.1 °C, a digital pressure measuring device (Heise model 901 A) with accuracy of ± 0.5 bar, a core holder, and a computer controlled high-pressure positive displacement pump with a volume resolution of 0.01 cc for pressurization. An Enerpac manual pump rated up to 815 bars to supply the overburden pressure around the core plug shielding by a lead sleeve was also available for use. Three sample cylinders with a volume of 500 cc each and maximum allowance pressure of 1020 bars to inject both live oil and injection fluids were also used. As shown in Fig. 1 a Back Pressure Regulator (BPR) system was used to maintain the pressure at the outlet of the core

Table 1: Physical properties of core samples used in the experiments.

Core sample	Average porosity (%)	Average Ka (md)	Average Swi (%)	Rock type	Core length (cm)	Core diameter (cm)
S1, S2, S3	12.5	8.0	0.20	Carbonate	31.5	3.8

holder at the desired value. Also a glassware separator was used in order to separate and measure the volume of the oil and gas recovered during the flooding experiments. A wet gas meter at barometric condition was used to measure the volume of the gas. The experiments were carried out with different flow rate of injection fluids at constant pressure, and the corresponding volumes of the hydrocarbons recovered during the experiments were measured. The experiments at each specified rate were repeated three times and the results were presented as the average of the experiments.

Samples

Live oil samples at reservoir pressure and at ambient temperature were supplied from one of the offshore reservoir in the south of Iran. In order to prepare the live oil sample, specified amount, of oil and gas at surface conditions were obtained and recombined according to the values for the Gas Oil Ratio (GOR) reported for the reservoir. Rock samples were obtained from the main outcrop of the reservoir and the core plugs were cut out in laboratory from the rock samples. As expounded the live fluid used in each scenario was prepared with recombination of oil and gas sample from the field separator with GOR of 330 Rcf/Rbbl at reservoir conditions.

Modeling

Analytical solutions to reservoir flow equations are only attainable after making assumptions with regard to the geometry, properties and boundary conditions that severely restrict the applicability of the solutions. For most real reservoir fluid flow problems, such simplifications are not valid. Therefore, we need to solve the equations numerically. Eclipse 100 is a numerical simulator utilizing standard finite difference equations. It can be used for lab scale modeling. It is a fully implicit, 3 - phase, and 3-D simulator and can be used to simulate one - phase, two - phase or three -phase systems. Two - phase options (oil/water, oil/gas, and gas/water) are solved as two component systems saving both computer storage and CPU time. Radial and Cartesian block-center options are available in 1-D, 2-D or 3-D. A 3-D radial option completes the circle allowing flow to take place across the 0/360 degree interface. Considering the fluid phases of oil, gas and water only, and substituting Darcy's equations and standard black oil fluid descriptions into the continuity equations, and the inclusion of the production / injection terms in the equations, will result in the flow equations for the three - phase. Both drainage and imbibition curves may be required in simulation of oil/gas/water systems, depending on the process considered. First, the core must be subdivided into a number of discrete grid blocks, and the time coordinate must be divided into discrete time steps. Then, the pressure in each block can be solved numerically for each time step.

The model used for this research is 3-dimensional with three - phase flowing and with single porosity in horizontal radial lab scale. All core samples and fluid properties used in the model are attributed to SIRRI-D, an Iranian offshore reservoir. Two wells inserted into the model, one well for production and one well alternatively used for gas and water injection. The production well control or outlet pressure from core was fixed based on reservoir pressure. The reservoir temperature was applied in the model. The lab scale laboratory data modeled for water flooding, gas flooding and WAG processes consisted of reservoir fluid modeling, lab modeling, and simulation of laboratory data at the lab scale. Eclipse 100 was used for above steps. Hereby the results are explained.

Reservoir Fluid Modeling

In reservoir fluid modeling, the reservoir fluid properties of Iranian off-shore field are used as shown in table 1. To study the phase behavior of the reservoir fluid the *Peng Robinson* EOS equation with 3 parameters along with the *Lohrenz-Bray-Clark* correction were used. Results of modeling were compared with the laboratory data. At temperature 370.3722 K the calculated bubble point pressure was 1561 pisa and the observed bubble point pressure 1560 psia.

Table 2: Physical properties of recombined oil, water and gas sample at reservoir conditions used in the experiments.

Reservoir temp.	°F	207
Gas solution in oil (RS)	SCF/STB	325-380
Oil volume factor (BO)	Res Vol./ Std Vol.	1.2686
Bubble point pressure	Psig	1545
Fluid viscosity @ Res. cond.	Cp	1.8
Oil density @ Res. cond.	Gr/cc	0.7786
Gas density @ Res. cond.	Gr/cc	0.00127
Water viscosity @ Res. cond.	Cp	0.9
Water volume factor (BW)	Res Vol./ Std Vol.	1.013
API		31.5

** Reservoir conditions:Temperature=207 °F, Pressure=4200 psia.*

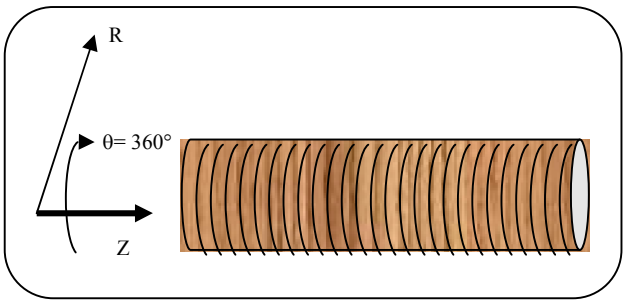

Fig. 2: Schematic figure for cylindrical core divided to 100 sections in Z direction.

Lab scale modeling

In lab scale modeling, cylindrical core divided to 100 cylindrical sections with dimension of 1×360×100 respectively for R, Θ and Z are shown in Fig. 2. Single porosity was considered in all the cases mentioned above.

RESULTS AND DISCUSSION

Tables 1 and 2 show, respectively, the physical properties of core samples and recombined reservoir fluid, water and gas samples at reservoir conditions. Table 1 shows the three samples of the core, S1, S2 and S3 with the same physical properties that were used during the experiments. Notably, the core samples were prepared according to the dimensions of the core flooding systems. A careful study of table 2 reveals that API for the oil sample is high enough to consider it as a light oil. As explained earlier to prepare the recombined and live oil sample, specified amounts of oil and gas at surface conditions were obtained and recombined based on the knowledge of the GOR values reported for the candidate offshore reservoir. The properties of the oil, water and gas are shown in table 2. These properties were measured at reservoir conditions.

Table 3 represents the analysis for the reservoir fluid composition, molecular weight and specific gravity of the hexane plus fraction. Tables 4 and 5, respectively, show the WAG process cycles for various injection rates at WAG ratio 1 and WAG ratio 2. The values reported in tables 4 and 5 were directly used in the modeling of the experimental results.

Table 6 shows the reservoir fluid properties of different phases. Theses properties are significant in both experimental and simulation studies.

Table 7 presents the experimental results of various EOR techniques obtained at different injection rates at 1.2 P.V injected. As can be seen the oil recovery factor obtained after implementation of different EOR technique changes with time. Also in table 7 the whole experimental results obtained from all scenarios can be compared at the same time. As shown in table 7 the maximum experimental oil recovery factor for injection rate of 0.1 cc/min and 1.2 P.V injected is attained using the WAG technique with WAG ratio 1 and 2. As mentioned before the uniform and stable frontal displacement can be obtained using the WAG process. The oil recovery factor using WAG technique with WAG ratio 2 is more than that in WAG ratio 1. As seen in Table 7 the maximum oil recovery factor for injection rate of 0.2 and 0.5 cc/min at 1.2 P.V injected is achieved using the WAG technique with WAG ratio 2. As shown the minimum oil recovery with all injection rates is observed using the gas flooding on the lab scale.

Figs. 3 to 14 show variations of the oil recovered, gas produced, water produced and oil recovery factors verses time obtained after implementation of the various EOR process, i.e., the WF, GI and the WAG on the lab scale. It would be worth noting that the rate of injection for each scenario was set to be 0.1, 0.2 and 0.5 cc/min, respectively. As can be seen from these figures the percentage of oil recovery increases with time. The results shown in Figs. 3 to 14 confirm that the WAG ratio set to 2 for all injection rates is optimal in producing highest percentage of oil recovery factor in WAG process. This can be justified by the fact that alternating use of gas and water as major injecting fluids can lead to a decrease in gas fingering phenomenon and to

Table 3: The reservoir fluid composition analysis.

Component	Mole per cent
Methane	23.45
Carbon Dioxide	2.05
Ethane	7.26
Propane	8.02
Iso Butane	1.92
Normal Butane	3.99
Iso Pentane	1.85
Normal Pentane	2.57
Hexane Plus	48.89
Total	100.00

Table 4: WAG process Cycles for various injection rate and WAG Ratio=1.

Injected fluid rate, (cc/ min)	For each cycle- WAG ratio=1.0		Number of cycles
	Water injection length, (min)	Gas injection length, (min)	
0.1	60	60	7
0.2	30	30	7
0.5	15	15	10

Table 5: WAG process Cycles for various injection rate and WAG Ratio=2.

Injected fluid rate, (cc/ min)	For each cycle- WAG ratio=2.0		Number of cycles
	Water injection length, (min)	Gas injection length, (min)	
0.1	80	40	7
0.2	40	20	7
0.5	20	10	10

Table 6: the reservoir fluid properties of different phases.

Fluid properties	Liquid	Vapor
Mole weight (g)	172.0104	22.4649
Z-factor	0.7936	0.8579
Viscosity (cp)	0.9684	0.0157
Density (g/cc)	0.7575	0.0915
Molar volume (cm^3/g.M)	227.0734	245.4817

approaching of the mobility ratio to unity in order to get the uniform and stable frontal displacement. In the case that the injection rate is considered to be 0.2 and 0.5 cc/min higher recovery factors can be obtained by implementation of the WF process compared to WAG ratio equal 1. Such observation can be plausibly explained that the higher injection rate of water can result in the bigger slug size of injection and thus, in turn, lead to increase the oil recovery. It should be stressed that higher injection rate of water cannot be tolerated in the field scale due the tremendous operation costs. As shown in table 7 the maximum percentage of oil recovery factor is attained using optimum injection volume, injection rate and WAG ratio by implementing the WAG scenario.

Also table 8 compares the results obtained from the experiments with those obtained from the simulation using the simulator. As can be observed from table 7 although the simulator slightly overestimates the experimental results, to a reasonable approximation, it is concluded that good agreement can be attained between the results of the simulator and those of the experiments.

Table 9 shows standard deviation of both experimental and simulation results for the amount of oil recovered after implementation of the various EOR techniques at different injection rates. As seen from Table 9 good agreement can be obtained using ECLIPSE 100 between the results of the simulator and those of the experiments.

CONCLUSIONS

The different EOR scenarios were both theoretically and experimentally studied on a lab scale for an Iranian offshore reservoir. The results showed that implementation of the WAG process with optimal injection volume, optimum rate of injection fluids and optimum WAG ratio can lead to a higher oil recovery comparing to the other alternating scenarios. It should be stressed that all the experiments were carried out at the same physical conditions and the same injection rates. The experiments were repeated three times and the results are the average of experimental data. It is also concluded that at very high injection rates the maximum recovery can be observed using the WF process while at moderate as well as operational injection rates the maximum recovery of oil is obtained by implementing the WAG process. The experimental results were compared with the results

Table 7: Experimental results for the amount of oil recovery factor after implementation of the various EOR techniques at 1.2 P.V injected and different injection rates.

Laboratory oil recovery % @ 1.2 P.V injected	Rate = 0.1 (cc/min)	Rate = 0.2 (cc/min)	Rate = 0.5 (cc/min)
Gas flooding	44.65	45.18	45.00
Water flooding	51.63	53.12	54.57
WAG injection- Ratio=1	53.16	52.13	53.90
WAG injection- Ratio=2	54.34	54.98	56.61
Simulation oil recovery % @ 1.2 P.V injected	Rate = 0.1 (cc/min)	Rate = 0.2 (cc/min)	Rate = 0.5 (cc/min)
Gas flooding	46.63	47.85	48.15
Water flooding	53.82	54.95	57.33
WAG injection- Ratio=1	48.03	47.92	49.02
WAG injection- Ratio=2	50.31	49.45	50.57

** Laboratory condition: Injection pressure = 4200 psig, Air bath temperature = 215 ^{o}F.*

Table 8: Standard deviation of experimental results for the amount of oil recovery factor after implementation of the various EOR techniques and different injection rates.

Scenario injection rate (cc/min)	WF	WAG ratio=1	WAG ratio=2	GI
0.1	16.274	13.182	13.795	14.101
0.2	16.894	14.077	14.870	11.505
0.5	14.552	11.932	12.743	13.164

Table 9: Standard deviation of simulation results for the amount of oil recovery factor after implementation of the various EOR techniques and different injection rates.

Scenario injection rate (cc/min)	WF	WAG ratio=1	WAG ratio=2	GI
0.1	12.765	3.25771	6.641	14.031
0.2	12.682	2.772	5.124	16.363
0.5	5.485	1.252	16.9	13.650

obtained from the simulator. It was concluded that good agreement exists between the results of the simulation and those of experiments.

Acknowledgments

We would like to express our gratitude to Sharif University of Technology and National Iranian Oil Company for financial support of the research project and permission to publish this paper.

Nomenclatures

M	Mobility ratio
R	Oil recovery
Ev	Vertical sweep efficiency
Eh	Horizontal sweep efficiency
Em	Microscopic displacement efficiency
kro	Oil relative permeability
krg	Gas relative permeability
µo	Oil viscosity
µg	Gas viscosity

Received : 14th January 2007 ; Accepted : 24th June 2007

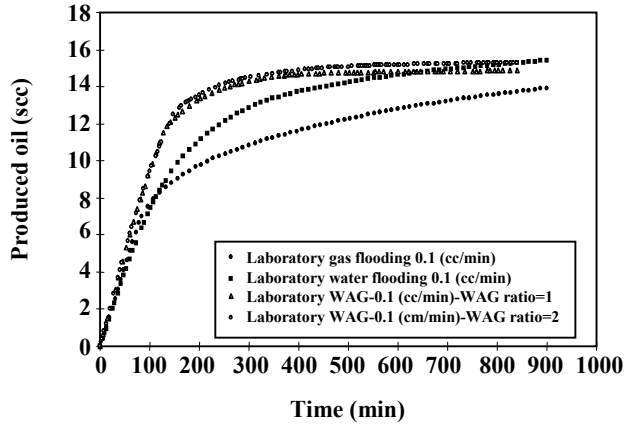

Fig. 3: Variation of the experimental amount of oil recovered after implementation of all scenarios respectively at injection rate of 0.1, 0.2, and 0.5 cc.min^{-1}.

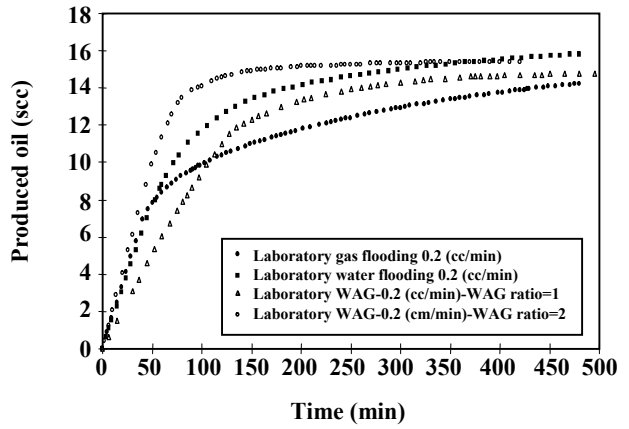

Fig. 4: Variation of the experimental amount of oil recovered after implementation of all scenarios respectively at injection rate of 0.1, 0.2, and 0.5 cc.min^{-1}.

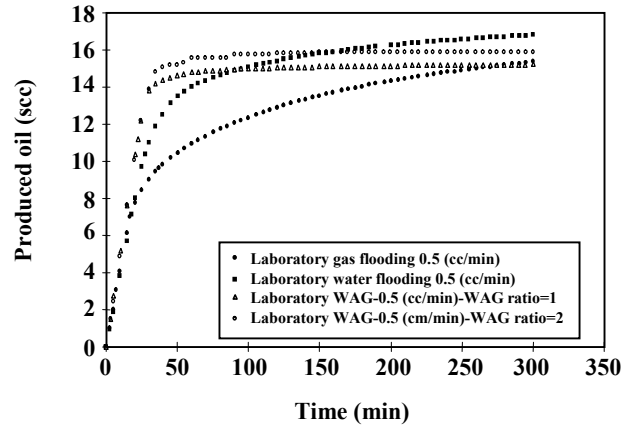

Fig. 5: Variation of the experimental amount of oil recovered after implementation of all scenarios respectively at injection rate of 0.1, 0.2, and 0.5 cc.min^{-1}.

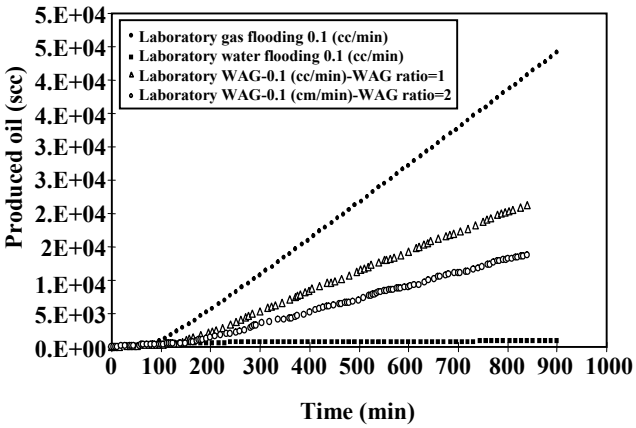

Fig. 6: Variation of the experimental amount of gas produced after implementation of all scenarios respectively at injection rate of 0.1, 0.2, and 0.5 cc.min^{-1}.

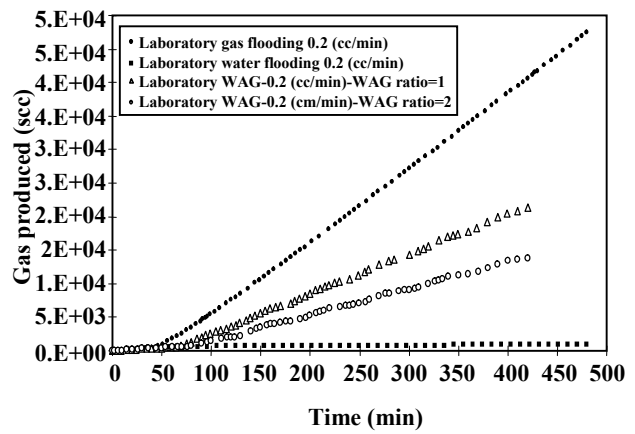

Fig. 7: Variation of the experimental amount of gas produced after implementation of all scenarios respectively at injection rate of 0.1, 0.2, and 0.5 cc.min^{-1}.

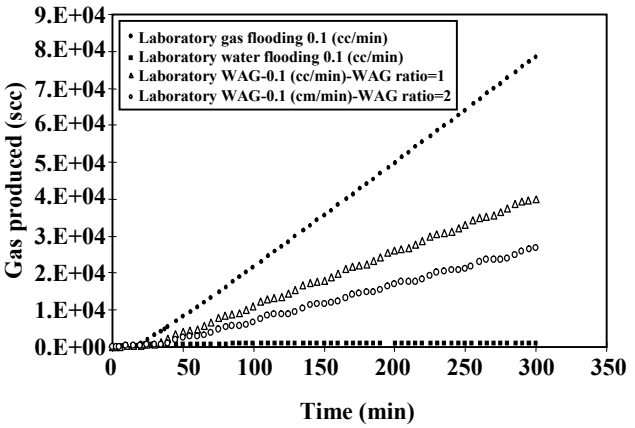

Fig. 8: Variation of the experimental amount of gas produced after implementation of all scenarios respectively at injection rate of 0.1, 0.2, and 0.5 cc.min^{-1}.

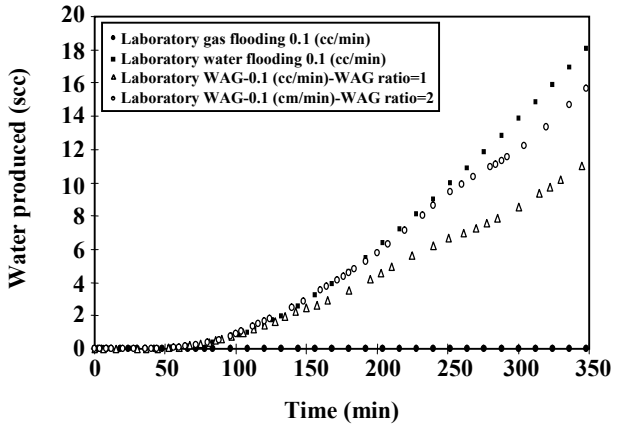

Fig. 9: Variation of the experimental amount of water produced after implementation of all scenarios respectively at injection rate of 0.1, 0.2, and 0.5 cc.min^{-1}.

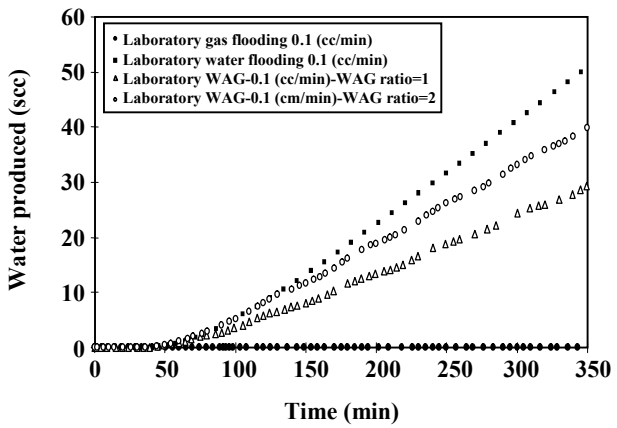

Fig. 10: Variation of the experimental amount of water produced after implementation of all scenarios respectively at injection rate of 0.1, 0.2, and 0.5 cc.min^{-1}.

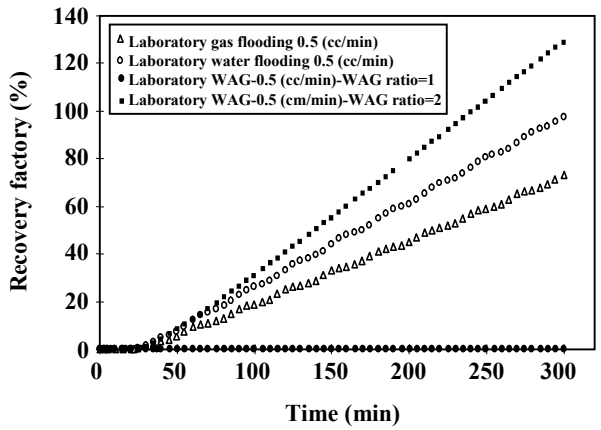

Fig. 11: Variation of the experimental amount of water produced after implementation of all scenarios respectively at injection rate of 0.1, 0.2, and 0.5 cc.min^{-1}.

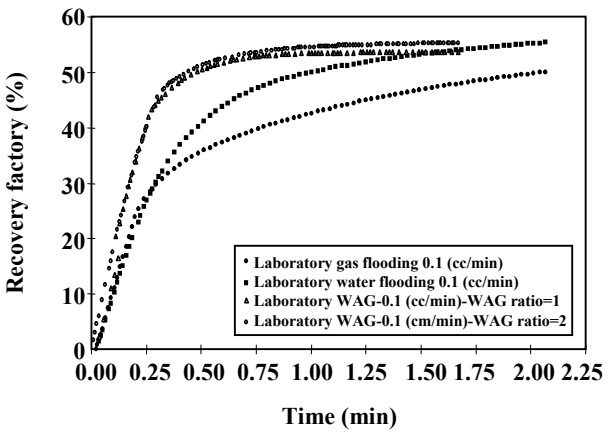

Fig. 12: Variation of the experimental amount of oil recovery factor after implementation of all scenarios respectively at injection rate of 0.1, 0.2, and 0.5 cc.min^{-1}.

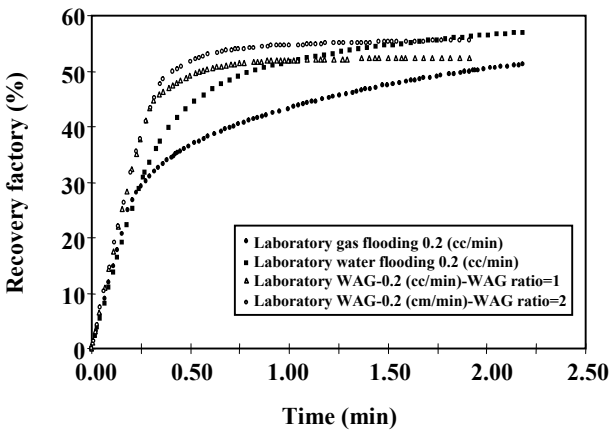

Fig. 13: Variation of the experimental amount of oil recovery factor after implementation of all scenarios respectively at injection rate of 0.1, 0.2, and 0.5 cc.min^{-1}.

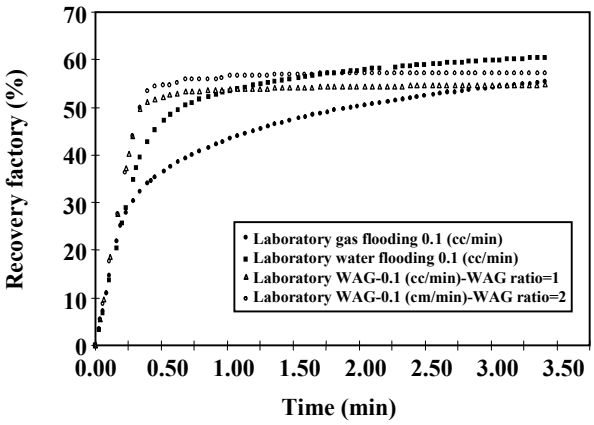

Fig. 14: Variation of the experimental amount of oil recovery factor after implementation of all scenarios respectively at injection rate of 0.1, 0.2, and 0.5 cc.min^{-1}.

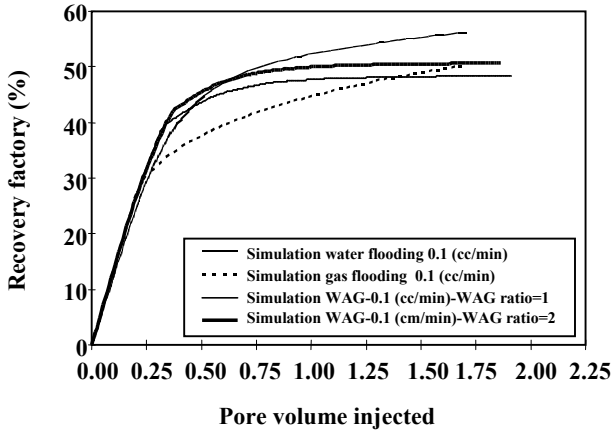

Fig. 15: Variation of the Simulation amount of oil recovery factor after implementation of all scenarios respectively at injection rate of 0.1, 0.2, and 0.5 cc.min^{-1}.

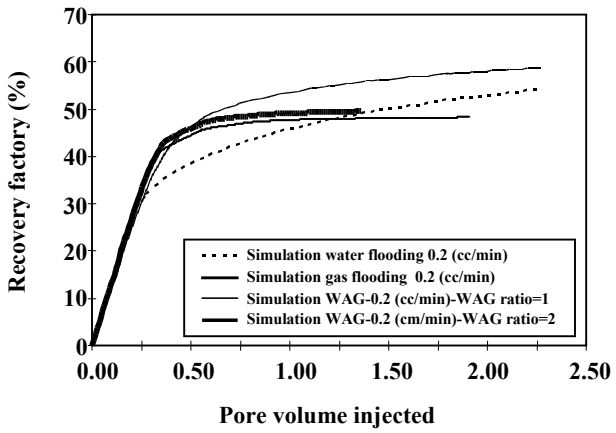

Fig. 16: Variation of the Simulation amount of oil recovery factor after implementation of all scenarios respectively at injection rate of 0.1, 0.2, and 0.5 cc.min^{-1}.

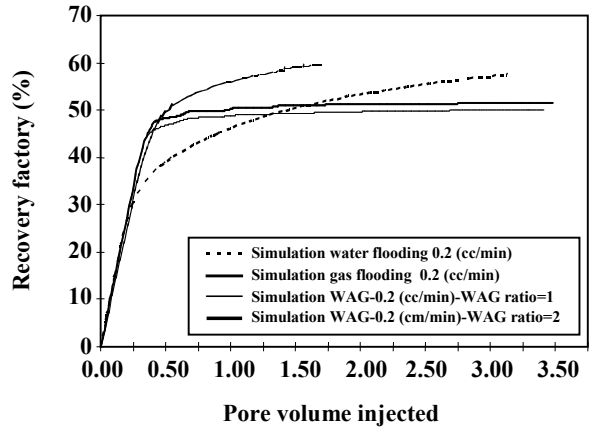

Fig. 17: Variation of the Simulation amount of oil recovery factor after implementation of all scenarios respectively at injection rate of 0.1, 0.2, and 0.5 cc.min^{-1}.

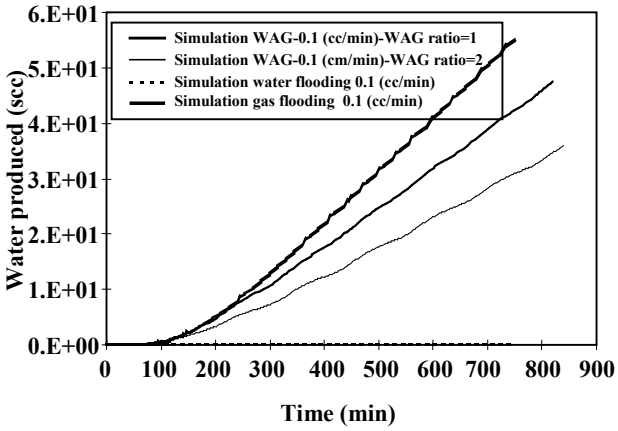

Fig. 18: Variation of the Simulation amount of water produced after implementation of all scenarios respectively at injection rate of 0.1, 0.2, and 0.5 cc.min^{-1}.

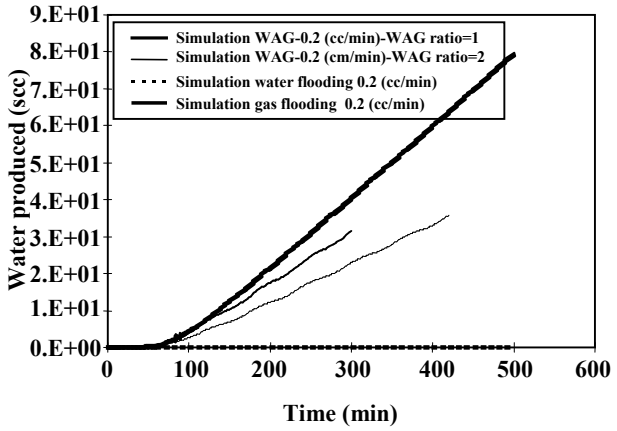

Fig. 19: Variation of the experimental amount of water produced after implementation of all scenarios respectively at injection rate of 0.1, 0.2, and 0.5 cc.min^{-1}.

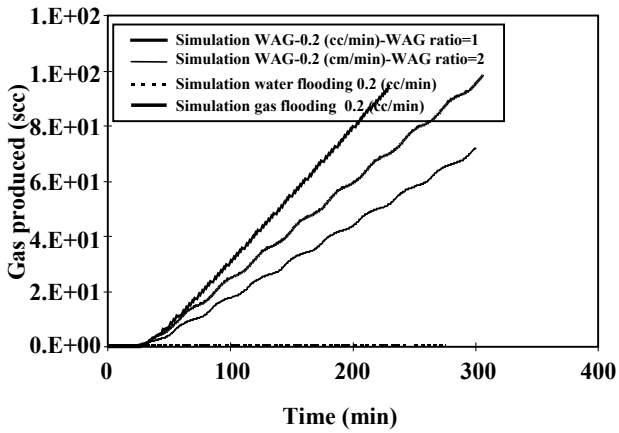

Fig. 20: Variation of the Simulation amount of water produced after implementation of all scenarios respectively at injection rate of 0.1, 0.2, and 0.5 cc.min^{-1}.

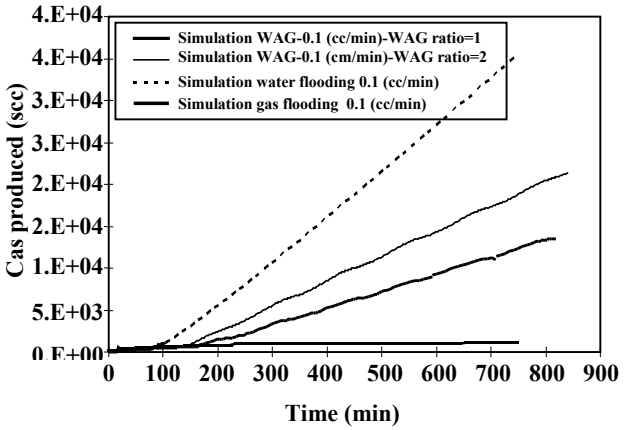

Fig. 21: Variation of the Simulation amount of gas produced after implementation of all scenarios respectively at injection rate of 0.1, 0.2, and 0.5 cc.min^{-1}.

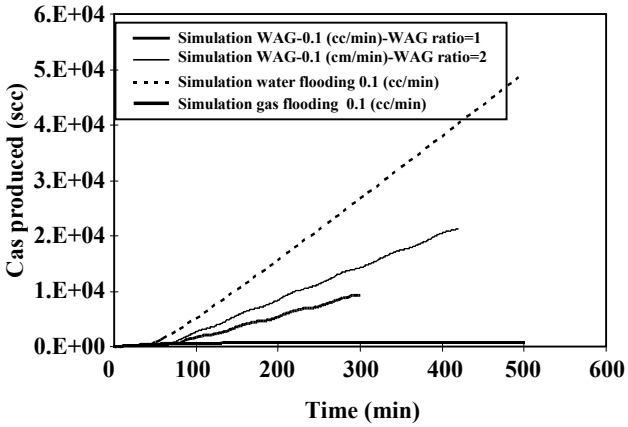

Fig. 22: Variation of the Simulation amount of gas produced after implementation of all scenarios respectively at injection rate of 0.1, 0.2, and 0.5 cc.min^{-1}.

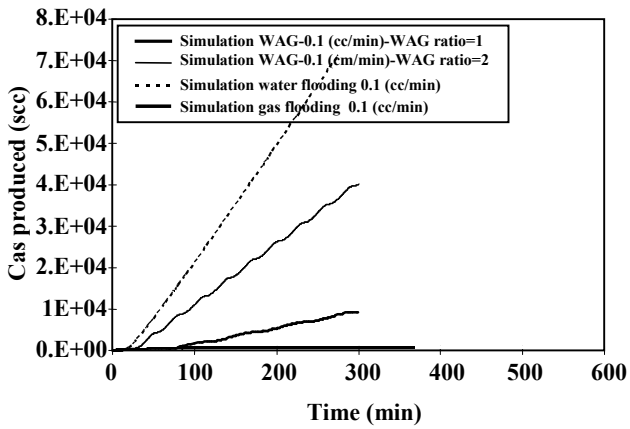

Fig. 23: Variation of the Simulation amount of gas produced after implementation of all scenarios respectively at injection rate of 0.1, 0.2, and 0.5 cc.min^{-1}.

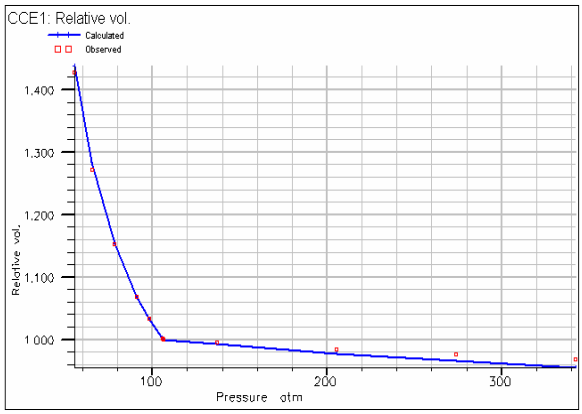

Fig. 24: Variation of the amount of relative volume after implementation of the model constructed based on PR EOS equation ○: Experimental data; —: results from model.

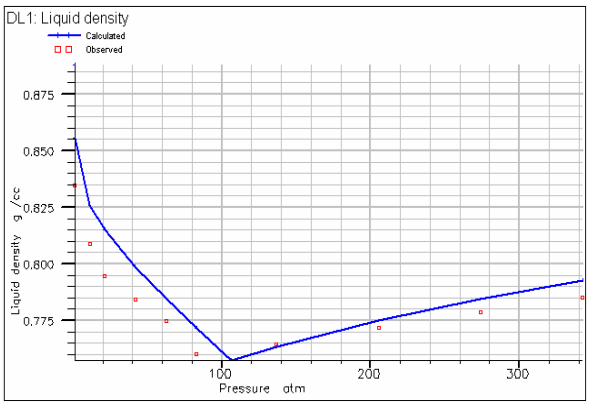

Fig. 25: Variation of the amount of liquid density after implementation of the model constructed based on PR EOS equation ○: Experimental data; —: results from model.

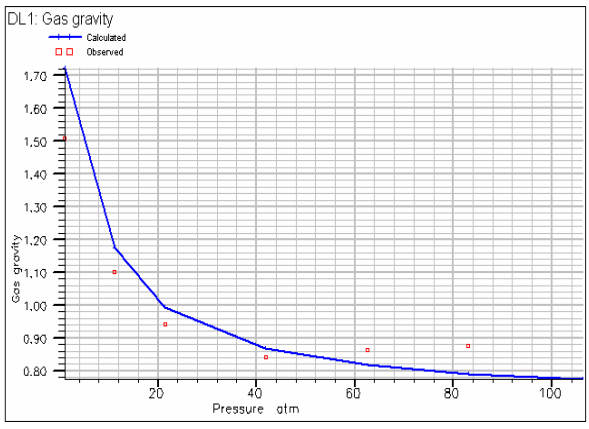

Fig. 26: Variation of the amount of gas density after implementation of the model constructed based on PR EOS equation ○: Experimental data; —: results from model.

REFERENCES

[1] Van Poollen, H.K., "Fundamentals of Enhanced Oil Recovery", PennWell Books, Tulsa, Oklahoma, (1980).

[2] Christensen, J. R., Stenby, E.H., Lyngby, DTU. and Skauge, Review of WAG Field Experience, SPE, Norsk Hydro ASA, Bergen, (1998).

[3] Nybraaten, G., Svorstoel, and Andfossen, P. O., WAG Pilot Evaluation for the Snorre Flcld, 7th European IOR, Moscow, Russia, (1993).

[4] Stenmark, H. and Andfossen, P. O., Snorre WAG Pilot-A Case Study, 8th European IOR, Vienna, Austria, (1996).

[5] Slotte, P. A., Stenrnark, H. and Aurd, T., Snorre WAG Pilot, *Norwegian Petroleum Directorate,* RUTH 1992 (1996).

[6] Jensen, J., Nesteby, H. and Slotte. P. A., Brage WAG Pilot, *Norwegian Petroleum Directorate,* RUTH 1992 (1996).

[7] Skauge, A. and Berg, E., Immiscible WAG Injection in the Fensfjord Formation of the Brage Oil Field, paper number 014, from EAGE, 9th European Symposium on Improved Oil Recovery, The Hague, 20-22 Oct. (1997).

[8] Skauge, A. and Aarra, M., Effect of Wettability on the Oil Recovery by WAG, Proceedings 7th European Symposium on Improved Oil Recovery, Moscow, (1993).

[9] Skauge, A. and Larsen, J. A., New Approach to Model the WAG Process, Proceedings, 15th International Energy Agency, Collaborative Project on Enhanced Oil Recovery, Workshop and Symposium, Bergen, Norway, 28-31 August, (1994).

[10] Magruder, J. B., Stiles, L.H. and Yelverton, T. D., "A Review for the Means San Andres Unit Full-Scale CO_2 Tertiary Project", SPE 17349, EOR Symposium, Tulsa, (1988).

[11] Prieditis, J., Wolle, C. R. and Notz, P. K., A Laboratory and Field Injectivity Study CO_2 WAG In the San Andres Formation of West Texas, SPE 22653, 66th ATCE, Dallas, (1991).

[12] Roper, M. K., Cheng, C. T., Varnon, J. E., Pope, G.A. and Sepehrnoori, K., Interpretation of a CO_2 WAG Injectivity Test in the San Anclres Formation Using a Compositional Simulator, SPE 24163, 8th EOR, Tulsa, (1992).

[13] Claridge, E. L., CO_2 Flooding Strategy in a Communicating Layered Reservoir, JPT Dec. (1982).

[14] Chase Jr., C.A. and Ttid, D., Numerical Simulation of CO_2 Flood Performance", SPE 10514, JPT, Dec. (1984).

[15] Stephenson, D.J., Graham, A.G. and Luhning R, W., Mobility Control Experience in the Joffre Viking Miscible CO_2 Flood, SPE Reservoir Engineering, Aug. (1993).

[16] Walker, J.W. and Turner, J. L., Performance of Seelington Zone 20B-07 Enriched-Gas-Drive Project, SPE 1884, JPT, April, (1968).

[17] Robie, Jr., D.R., Roedell, J.W. and Wackowski, R. K., Field Trial of Simultaneous Injection of CO_2 and Water, Rangely Weber Sand Unit, Colorado (1998).

[18] Ma, T. D., Rugen, J.A. and Stoisits, R. F., Simultaneous Water and Gas Injection Pilot at the Kuparuk River Field, Reservoir Impact, SPE 30726, ATCE, Dallas, (1995).

[19] Hong, K.C. and Stevens, C. E., Water-Alternating-Steam Process Improves Project Economics at West Coalinga, SPE Res. Eng., November, Texas (1992).

[20] Skauge, A., Simulation Studies of WAG Using Three - Phase Relative Permeability Hysteresis Models, Paper Number 015, Proceeding from EAGE, 9th European Symposium on Improved Oil Recovery, The Hague, 20-22 Oct. (1997).

[21] Helm, L.W., Propane-Gas-Water Miscible Floods In Watered-Out Areas of the Adena Field, SPE 3774, JPT Oct., (1972).

[22] Watts, R. J., Conner, W. D., Wasson, J.A. and Yost, A.B., CO_2 Injection for Tertiary Oil Recovery, Granny's Creek Field, Clay County, West Virginia, SPE 10693, 3rd EOR, Tulsa, (1982).

[23] Dyes, A, B., Bensimina, A., Saadi, A.M. and Khelil, C., Alternate Injection of HPG and Water, Two Well Pilot, SPE 4082, 47th Annual Fall Meeting, San Antonio, Texas, (1972).